

Suppression of Iron Catalyzed Free Radical Generation by Iron Tyrosinate Protein Models

Manabu Kitazawa and Keiji Iwasaki¹

Central Research Laboratories, Ajinomoto Co., Inc., Suzuki-cho 1-1, Kawasaki-ku, Kawasaki, Kanagawa 210, Japan

Received January 31, 1996

Novel antioxidants, N-(2-Hydroxy-1-naphthal)amino acids which mimic iron proteins, have been intensively studied for suppressive effect on iron-catalyzed free radical generation. These compounds exhibit inhibition of the Fenton reaction in electron spin resonance assessment. In addition, it is shown that the compounds inhibit iron-induced peroxidation by thiobarbituric acid test. Since these antioxidants form stable complexes with Fe^{3+} , this antioxidative activity is expected to be derived from sequestration of catalytic iron. © 1996 Academic Press, Inc.

In recent years, oxidative stress and its relationship to human disease have become an important research area. Oxidative stress in cells and tissues leads to increased generation of oxygen free radicals (1). The reactions of these reactive oxygen species with DNA, protein, and membrane lipids are associated with many human diseases such as ischaemia/reoxygenation injury, inflammation, ageing, and cancer (2,3). These deleterious biological free radical reactions are catalyzed by transition metals, particularly iron. In the case of iron, the reaction is known as the Fenton reaction (Fig. 1) (4,5). Catalytic iron is thought to be released from proteins such as transferrin, lactoferrin, and ferritin, under oxidative stress due to high oxygen tension and/or UV light (6). However, in living systems the iron is transported and stored in proteins in order not to catalyze free radical formation. Therefore, sequestering iron by chelating agents is one of the effective approaches to prevent the generation of deleterious free oxygen radicals (1,4). It has been reported that DFO, which is a strong iron chelating agent, shows protective effect on many pathological conditions (7). However, its extremely high affinity for iron in iron-storage proteins results in its not only trapping the released iron but also removing stored iron (8). This may cause undesirable side-effects, and the clinical applications of DFO are limited (7, 9). EDTA, which is a commonly used iron chelator, can not completely occupy the iron-binding site, hence the EDTA-iron complex is ineffective in suppressing the formation of reactive oxygen species, even when the chelator is in large excess (10).

For a molecular design suitable for suppression of the catalytic activity of free iron in the body, it is reasonable to mimic the binding site of iron sequestering proteins. The iron-binding ability of compounds which mimic iron proteins is thought to be equivalent to that of iron proteins because of the structural similarity of iron-binding site. Moreover, with respect to the occupation of the iron-binding site and catalytic states of iron, the artificial complexes seem to be analogous to iron proteins. Therefore, it is expected that the mimetic compounds trap only released iron and prevent the trapped iron from catalyzing free radical reactions. According to this principle for molecular design, our interest was focused on iron tyrosinate protein models (11). Here we report the suppressive effect of protein mimetic compounds on iron-induced free radical generation. N-(2-hydroxy-1-naphthal)amino acid has been found to show an antioxidant effect *in vitro* and a

¹ To whom correspondence should be addressed. Fax: +81-44-244-8938.

Abbreviations: ESR, electron spin resonance; TBA, thiobarbituric acid; UV, ultraviolet; DFO, desferrioxamine; EDTA, ethylenediaminetetraacetic acid; DMPO, 5,5-dimethyl-1-pyrroline-N-oxide; DMPO-OH, DMPO spin adducts with hydroxyl radicals; MDA, malon-dialdehyde; HEDT, N-hydroxyethyl-ethylenediaminetriacetic acid; NTA, nitrilotriacetic acid; HEPES, 4-(2-hydroxyethyl)-1-piperazine ethanesulfonic acid.

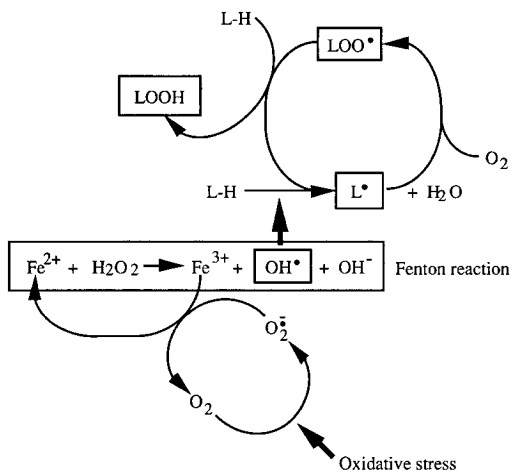


FIG. 1. Generalized mechanism for iron-induced reactive oxygen species generation and lipid peroxidation in cells and tissues (5).

moderate iron-binding ability. In this paper we describe effectiveness of the model compounds whose amino acid residue are glycine and L-serine (**1** and **2**, respectively) (Fig. 2) as antioxidants.

MATERIALS AND METHODS

Chemicals. All reagents were used without purification. 2-Hydroxy-1-napthaldehyde, TBA, EDTA, HEDT, and NTA were purchased from Tokyo Kasei Co., Inc. (Tokyo, Japan). DMPO was from Labotec Co., Inc. (Tokyo, Japan). Ferrous sulfate (heptahydrate), ferrous ammonium sulfate (hexahydrate), DFO, and HEPES were from Sigma Chemical Co. (St. Louis, MO). Hydrogen peroxide (30%, w/v), trichloroacetic acid, ferrous nitrate (nonahydrate), and potassium nitrate were from Junsei Kagaku Co., Inc. (Tokyo, Japan).

Synthesis. The model compounds (**1** and **2**) were synthesized by Schiff base condensation of corresponding amino acid with 2-hydroxy-1-napthaldehyde using a conventional method (Fig. 2) (12) and afforded in 80–90% yield as yellow needle crystals. Mass spectra were determined with a JEOL JMS-DX300 spectrometer. ^1H NMR spectra were recorded with a Varian XL-300 spectrometer, and the chemical shifts (δ) in parts per million (ppm) units were referenced to the TMS internal standard. N-(2-hydroxy-1-napthal)glycine (**1**): FAB-MS m/z 230 [(M+H) $^+$]. ^1H NMR (DMSO- d_6) δ = 9.06 (s, 1 H), 8.01 (d, J = 8.6 Hz, 1 H), 7.74 (d, J = 8.6 Hz, 1 H), 7.63 (d, J = 8.6 Hz, 1 H), 7.43 (t, J = 8.6 Hz, 1 H), 7.20 (t, J = 8.6 Hz, 1 H), 6.74 (d, J = 8.6 Hz, 1 H), 4.48 (s, 2 H). Anal. Calcd for $\text{C}_{13}\text{H}_{11}\text{NO}_3$: C, 68.11; H, 4.84; N, 5.96%. Found: C, 68.24; H, 4.84; N, 6.11%. N-(2-hydroxy-1-napthal)-L-serine (**2**): FAB-MS m/z 260 [(M+H) $^+$]. ^1H NMR (DMSO- d_6) δ = 9.05 (s, 1 H), 8.08 (d, J = 8.5 Hz, 1 H), 7.73 (d, J = 9.2 Hz, 1 H), 7.63 (d, J = 8.5 Hz, 1 H), 7.42 (t, J = 8.5 Hz, 1 H), 7.20 (t, J = 8.5 Hz, 1 H), 6.82 (d, J = 9.2 Hz, 1 H), 4.51 (t, J = 3.8 Hz, 1 H), 3.88 (d, J = 3.8 Hz, 2 H). Anal. Calcd for $\text{C}_{14}\text{H}_{13}\text{NO}_4$: C, 64.85; H, 5.05; N, 5.40%. Found: C, 64.71; H, 5.01; N, 5.31%.

Iron-induced hydroxyl radical formation assay. The inhibition of iron-induced hydroxyl radical formation was determined by using ESR spin trapping technique in combination with DMPO (13). DMPO-OH was obtained from the Fenton reaction system which contained 0.30 mM FeSO_4 , 75 mM DMPO, and 0.30 mM H_2O_2 in 100 mM phosphate buffer solution (pH = 7.4) with the test compound (0.30 mM) or vehicle. This mixture was transferred to a JEOL LLC-04B flat cell and the ESR spectrum was recorded 60 sec after addition of H_2O_2 . The spin adducts formed in the reaction system were detected using a JEOL JES-RE1X spectrometer at room temperature. Instrumental conditions were as follows: microwave power, 8 mW; modulation amplitude, 0.1 mT; time constant, 0.01 sec; sweep scan rate, 0.17 mT/sec; central field, 348 mT; scan

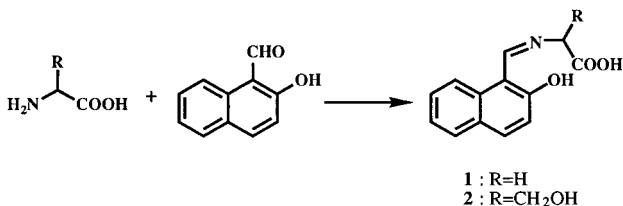


FIG. 2. Reaction scheme of the synthesis of the model compounds (**1** and **2**).

range, 10 mT; gain 1×100 . The signal intensities were evaluated by the peak height of the second signal of the quartet of DMPO-OH using MnO signal as a reference.

Iron-induced lipid peroxidation assay. The effectiveness of the compounds against iron-induced lipid peroxidation was evaluated by using a homogenate of mouse brain. Male C57BL/6 mouse (7 weeks) (Charles River Japan Co., Inc, Atsugi, Japan) were killed by cervical dislocation and brain homogenates were prepared in a ratio of 1 g of wet brain to 100 ml of 20 mM phosphate buffer solution (pH=7.4) by using a homogenizer, so as to contain approximately 0.5 mg of protein in 1 ml suspension. The content of protein was determined by the biuret method (14). Lipid peroxidation was determined by measuring TBA reactive substances, that is TBA-MDA adducts (15,16). A typical procedure was as follows: After incubation of 1.0 ml of the reaction mixture containing 1.0 mM **1** or **2** and 0.1 mM $\text{Fe}(\text{NH}_4)_2(\text{SO}_4)_2$ at 37°C for 30 min, 1.0 ml of 0.375 wt% TBA in 15 wt% trichloroacetic acid-250 mM hydrochloric acid was added, and the mixture heated at 90°C for 15 min. After cooling, TBA-MDA adducts were extracted with 2.0 ml of *n*-butanol. The absorbance of the organic layer is measured at 535 nm using a Hitachi 320 spectrophotometer equipped with a quartz cell of 10 mm optical path length.

Ferric ion (Fe^{3+}) binding assay. The stoichiometry of binding of **1**- or **2**-to- Fe^{3+} was determined by continuously measuring the increase in absorbance at 520 nm due to the complex formation (Fig. 3). Samples containing 0–0.45 mM $\text{Fe}(\text{NO}_3)_3$, 0.3 mM **1** or **2**, and 100 mM KNO_3 in 50 mM HEPES buffer solution (pH=7.4) were prepared. The stability constant ($\log K$) of **2**-to- Fe^{3+} complex was determined by measuring the equilibrium constant (K_{ex}) in a ligand exchange reaction. The ligand exchange reaction was followed by measuring the decrease in the absorbance at 520 nm for **2**-to- Fe^{3+} complex (Fig. 3). Ligand as references such as EDTA, HEDT, or NTA was added to the mixtures that **2**-to- Fe^{3+} complex was formed. The solution contained 0.14 mM $\text{Fe}(\text{NO}_3)_3$, 0.3 mM **2**, 0.15 mM ligand, and 100 mM KNO_3 in 50 mM HEPES buffer solution (pH=7.4). Each measurement for absorbance was carried out at 25°C in an apparatus described previously.

RESULTS

The model compounds (**1** and **2**) can be easily isolated and are physically and chemically stable compared with N-salicylidene amino acids that are structurally and functionally considered as iron tyrosinate protein models (11). Since N-salicylidene amino acids easily decompose to salicylaldehyde and amino acids in the absence of iron ion, they are unsuitable for use in clinical applications as iron chelators. Possibly the stability of **1** and **2** is due to the extended π -electron conjugate system in the molecules.

In evaluation of inhibition of iron-induced hydroxyl radical formation, trapping of generated hydroxyl radicals by **1** or **2** can be neglected since a large excess of DMPO was used. No signal corresponding to DMPO-OH was observed at all without DMPO and/or iron ion. Therefore, the significant decreases in the spectra of DMPO-OH in Fig. 4 (b) and (c) show the decrease of the hydroxyl radical generation by suppressing the catalytic activity of iron. Inhibition of the Fenton reaction by **1** and **2** is shown in Table 1.

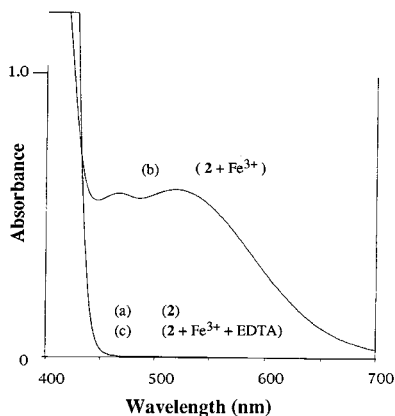


FIG. 3. Optical spectra of solutions containing the model compound (**2**). The spectra of **2** in the absence of Fe^{3+} (a), **2** in the presence of Fe^{3+} (**2**-to- Fe^{3+}) (b), and iron removal from **2**-to- Fe^{3+} by EDTA (c). Spectra (b) and (c) were obtained one day after preparing the solutions to reach the equilibrium. Spectra (a) and (c) are overlapped.

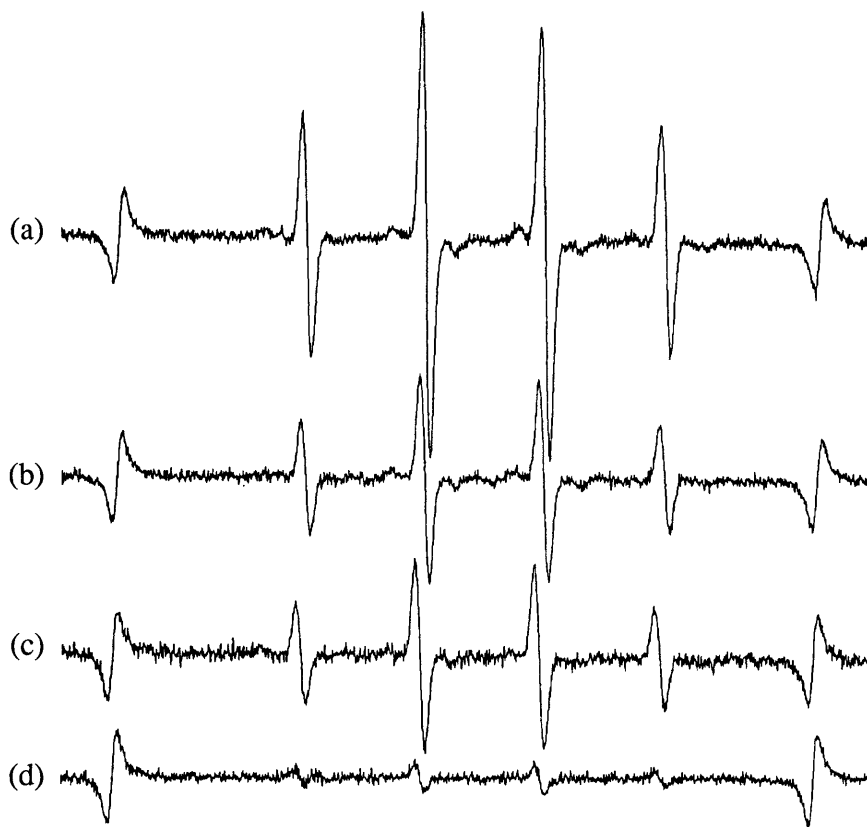


FIG. 4. Effect of the model compounds (**1** and **2**) on iron-induced hydroxyl radical formation. ESR spectrum of DMPO-OH spin adduct obtained from Fenton reaction system in the absence of antioxidants (a) and in the presence of **1** (b), **2** (c), and DFO (d).

The effectiveness of **1** and **2** were also shown in the iron-induced lipid peroxidation assay (Table 1). Although reactants (amino acid and 2-Hydroxy-1-naphtaldehyde) and product (**1** or **2**) in Fig. 2 bear an equilibrium relationship, there is a difference in the effectiveness between two forms (Fig. 5). The condensed formation of **1** or **2** prior to its addition to the assay mixture is advantageous for inhibition of the lipid peroxidation. This result suggests that the equilibrium is slowly reached.

The stoichiometry of binding was found to be 2:1 in both **1**- and **2**-to- Fe^{3+} complexes, because inflection points for absorbance vs. ratio of iron ($[\text{Fe}^{3+}]/[\textbf{1 or 2}]$) clearly appeared at the ratio value of 0.48–0.51 at 520 nm (Fig. 6), which is the λ_{max} of the complexes (Fig. 3). In the ligand exchange

TABLE 1
Summary of Antioxidative Activity of the Model Compounds (**1** and **2**)

Compound tested	ESR assessment		TBA assessment	
	Inhibition	50% Inhibition concentration (IC ₅₀)	Inhibition	50% Inhibition concentration (IC ₅₀)
1	57%	0.23 mM	61%	0.67 mM
2	60%	0.21 mM	80%	0.40 mM
DFO	94%	0.08 mM	81%	0.09 mM

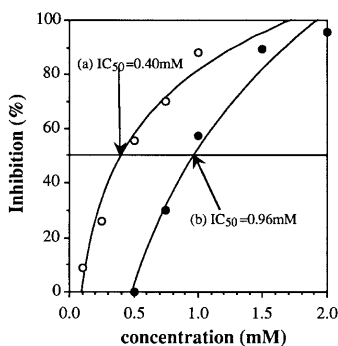


FIG. 5. Effect of the model compound (**2**) on iron-induced lipid peroxidation. Concentration dependence of the effectiveness by **2** (condensed form) (a) and L-serine and 2-Hydroxy-1-napthaldehyde (noncondensed form) (b).

reaction, values of the exchange ratio for EDTA, HEDT, and NTA were measured to be 1.00, 0.78, and 0.04, respectively. The equilibrium constant (K_{ex}) is described by

$$K_{\text{ex}}(\mathbf{2} \text{ vs } \mathbf{L}) = \frac{[\text{Fe} \cdot \mathbf{L}][\mathbf{2}]^2}{[\text{Fe} \cdot \mathbf{2}]_2[\mathbf{L}]}$$

where L is the ligand used as reference. Each concentration in the formula can be expressed by the initial concentration of **2**, L and Fe^{3+} ($[\mathbf{2}]_0$, $[\mathbf{L}]_0$ and $[\text{Fe}]_0$, respectively) shown in Materials and Methods and by the exchange ratio (R) as follows: $[\text{Fe} \cdot (\mathbf{2})_2] = (1-R)[\text{Fe}]_0$, $[\mathbf{L}] = [\mathbf{L}]_0 - R[\text{Fe}]_0$, $[\text{Fe} \cdot \mathbf{L}] = R[\text{Fe}]_0$ and $[\mathbf{2}] = [\mathbf{2}]_0 - 2(1-R)[\text{Fe}]_0$. Therefore, the values were led to as follows: $K_{\text{ex}}(\mathbf{2} \text{ vs. HEDT}) = 4.91 \times 10^{-3} \text{ M}$ and $K_{\text{ex}}(\mathbf{2} \text{ vs. NTA}) = 2.81 \times 10^{-7} \text{ M}$.

DISCUSSION

Since **1** and **2** form stable complexes with Fe^{3+} and inhibit iron-induced lipid peroxidation, the compounds are expected to suppress free radical reactions by sequestering catalytic iron in the body, in light of the case of DFO. We have confirmed formation of 2:1 complexes of **1** or **2** to Fe^{3+} . Since the hydroxy group in the aromatic ring and the carboxylate and amino groups in the amino acid residues in the ligands can coordinate to Fe^{3+} , it is expected that all the six coordination sites of Fe^{3+} are occupied with two ligand molecules. Thus the iron complex no longer catalyzes the Fenton reaction because of the absence of the catalytic site. The mechanism for its antioxidative activity is suggested to be the stabilization of Fe^{3+} to which Fe^{2+} is rapidly converted by auto-oxidation (17). In preliminary studies for $\log K$ of 2-to- Fe^{3+} complex, we estimated the value to be 22.1–22.5 on the basis of the experimental K_{ex} values, using $\log K$ values of HEDT- and NTA-to-

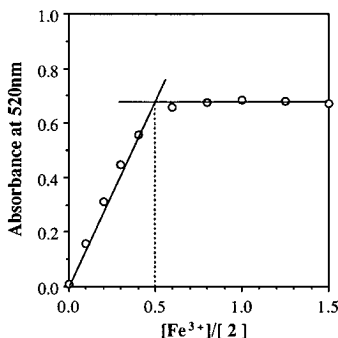


FIG. 6. Stoichiometry study for binding ratio in **2**-to- Fe^{3+} .

Fe^{3+} complex of 19.8 and 15.9, respectively (18). This is larger than that of iron proteins ($\log K = 16\text{--}18$) (19) but much smaller than that of DFO ($\log K = \sim 30$) (20). The moderate affinity of compound 2 for iron, compared with DFO's, should avoid the undesirable side-effects caused by trapping stored iron. These suitable properties as an antioxidant are thought to be derived from the similarity in mechanism of iron-binding to that of iron proteins. The iron tyrosinate protein models introduces novel approaches to the molecular design for antioxidants.

ACKNOWLEDGMENT

The authors thank Professor Barry Halliwell of the Department of Biochemistry, University of London King's College for his helpful comments on our study.

REFERENCES

- Halliwell, B., and Gutteridge, J. M. C. (1989) *Free Radicals in Biology and Medicine*, Clarendon Press, Oxford, England.
- Halliwell, B. (1991) *Drugs* **42**, 569.
- Stadtman, E. R. (1992) *Science* **257**, 1220.
- Miller, D. M., Buettner, G. R., and Aust, S. D. (1990) *Free Radical Biol. Med.* **8**, 95.
- Ogura, R., Sugiyama, M., Nishi, J., and Haramaki, N. (1991) *J. Invest. Dermatol.* **97**, 1044.
- Trenam, C. W., Blake, D. R., and Morris, C. J. (1992) *J. Invest. Dermatol.* **99**, 675.
- Halliwell, B. (1989) *Free Radical Biol. Med.* **7**, 645.
- Kretchmar, S. A., Craig, A., and Raymond, K. N. (1993) *J. Am. Chem. Soc.* **115**, 6758.
- Bergeron, R. J., Wiegand, J., Dionis, J. B., Egli-Karmakka, M., Frei, J., Huxley-Tencer, A., and Peter, H. H. (1991) *J. Med. Chem.* **34**, 2072.
- Dean, R. T., and Nicholson, P. (1994) *Free Rad. Res.* **20**, 83.
- Casella, L., Gullotti, M., Pintar, A., Messori, L., Rockenbauer, A., and Gyor, M. (1987) *Inorg. Chem.* **26**, 1031.
- McIntire, F. C. (1947) *J. Am. Chem. Soc.* **69**, 1377.
- Buettner, G. R., and Mason, R. P. (1990) *Methods Enzymol.* **186**, 127.
- Gornall, A. G., Bardawill, C. J., and David, M. M. (1949) *J. Biol. Chem.* **177**, 751.
- Buege, J. A., and Aust, S. D. (1978) *Methods Enzymol.* **52**, 302.
- Ohkawa, H., Ohishi, N., and Yagi, K. (1979) *Anal. Biochem.* **95**, 351.
- Miller, D. M., Spear, N. H., and Aust, S. D. (1992) *Arch. Biochem. Biophys.* **295**, 240.
- Akiyama, M., Katoh, A., Iijima, M., Takagi, T., Natori, K., and Kojima, T. (1992) *Bull. Chem. Soc. Jpn.* **65**, 1356.
- Hojo, N., Shirai, H., and Kaneko, M. (1991) Seitai to Kinzoku-ion (Living Bodies and Metallic Ion), Gakkai Shuppan Center, Tokyo, Japan.
- Anderegg, G., L'Eplattenier, F., and Schwarzenbach, G. (1963) *Helv. Chim. Acta* **156**, 1409.